Threshold Fluctuations in an *N* Sodium Channel Model of the Node of Ranvier

J. T. Rubinstein
Department of Otology and Laryngology, Harvard Medical School and Cochlear Implant Research Laboratory, Massachusetts Eye and Ear Infirmary, Boston, Massachusetts 02114 USA

ABSTRACT Computer simulations of stochastic single-channel open-close kinetics are applied to an *N* sodium channel model of a node of Ranvier. Up to 32,000 voltage-gated sodium channels have been simulated with modified amphibian sodium channel kinetics. Poststimulus time histograms are obtained with 1000 monophasic pulse stimuli, and measurements are made of changes in the relative spread of threshold (RS) with changes in the model parameters. RS is found to be invariant with pulse durations from 100 μs to 3 ms. RS is approximately of inverse proportion to $\sqrt{N}$. It decreases with increasing temperature and is dependent on passive electrical properties of the membrane as well as the single-channel conductance. The simulated RS and its independence of pulse duration is consistent with experimental results from the literature. Thus, the microscopic fluctuations of single, voltage-sensitive sodium channels in the amphibian peripheral node of Ranvier are sufficient to account for the macroscopic fluctuation of threshold to electrical stimulation.

INTRODUCTION

Before the advent of single-channel recording and the recognition that substantial membrane noise is due to the random, open-close kinetics of large numbers of ionic channels (DeFelice, 1981; Hille, 1992), fluctuation of excitability was of great experimental and theoretical interest (Blair and Erlanger, 1933; Pecher, 1939; Poussart, 1965; Ten Hoopen and Verveen, 1963; Verveen, 1962; Verveen and Derksen, 1965; Verveen and Derksen, 1968). Verveen and his colleagues systematically studied fluctuation of excitability with electrical stimulation in a large number of single fibers of differing size. They concluded that the probability of firing, as a function of stimulus current, for a given fiber could be described with a Gaussian distribution function (Ten Hoopen and Verveen, 1963; Verveen, 1962; Verveen and Derksen, 1965). Verveen defined the "threshold" as the stimulus intensity at which the fiber fired 50% of the time. He also defined the relative spread of threshold (RS) as the coefficient of variation, i.e., the standard deviation divided by the mean of the Gaussian for that fiber. Although threshold varied both with stimulus parameters and across fibers, RS was independent of stimulus parameters and appeared to be an inherent property of the fiber with a strong dependence on fiber diameter (Verveen, 1962).

Verveen postulated that each fiber had an inherent noise source that was an order of magnitude greater in intensity than could be accounted for by thermal noise. Subsequent developments in fluctuation analysis and single-channel recording suggested that the random, open-close kinetics of ionic channels were a significant source of membrane noise (Hille, 1992). In an elegant theoretical treatise, Lecar and Nossal used phase-plane analysis to define the relationship between idealized membrane noise and threshold fluctuation (Lecar and Nossal, 1971). Using their equations and his own precise measurements of sodium channel fluctuations, Sigworth (1980) demonstrated that the microscopic sodium channel noise was sufficient to account for the macroscopic threshold fluctuations measured earlier by Verveen.

Clay and DeFelice further defined the relationship between single-channel kinetics and fluctuation in excitability by developing a numerical technique to simulate a population of voltage-sensitive channels not under voltage-clamp (Clay and DeFelice, 1983). The largest number of sodium channels simulated was 640. Although they estimated the coefficient of variation of spike latency and documented its inverse relation to $\sqrt{N}$, they did not publish post-stimulus time (PST) histograms or attempts to estimate RS.

In this paper, the technique of Clay and DeFelice is applied to a model of the amphibian node of Ranvier using modified Frankenhauser-Huxley kinetics (Frankenhauser and Huxley, 1964; Schwarz and Eikhof, 1987). The simulations include up to 32,000 sodium channels, and PST histograms are obtained in response to 1000 monophasic rectangular pulse stimuli. Input-output functions are obtained and RS calculated for a range of stimulation and membrane parameters. These theoretical results are very similar to experimental PST histograms and measurements of RS from the amphibian peripheral nerve (Poussart, 1965; Verveen and Derksen, 1965). The conclusions are similar to those of Sigworth (1980): that the microscopic fluctuations of the voltage-dependent sodium channel are sufficient to account for the macroscopic fluctuation of threshold. The numerical approach of Clay and DeFelice (1983), however, represents individual channel noise with greater physiologic precision than these earlier analytic approximations. Rather than modeling a population of channels with idealized statistics

Received for publication 23 May 1994 and in final form 12 October 1994.
Address reprint requests to Dr. J. T. Rubinstein, Department of Otolaryngology University of Iowa Hospitals & Clinics, 200 Hawkins Drive, Iowa City, IA 52242. Tel.: 319-356-2173; Fax: 319-356-4547; E-mail: jay-rubinstein@uiowa.edu.

0006-3495/95/03/779/07 $2.00

and phase-plane analysis, each channel is individually represented in a numerical solution of the stochastic, nonlinear differential equation that describes the time-varying behavior of the node.

MATERIALS AND METHODS

Theory

Consider the model for the node of Ranvier illustrated in Fig. 1. A "large" population of N voltage-dependent sodium channels is placed in parallel with the nodal leak resistance R_m and membrane capacitance C_m. The membrane potential, a time-varying random variable $\tilde{V}(t)$, is obtained by numerical solution of the differential equation

$$i_{app}(t) = C_m \frac{d\tilde{V}}{dt} + \frac{\tilde{V}}{R_m} + \gamma_{Na}\tilde{n}_{Na}(t)\{\tilde{V} - E_{Na}\}, \quad (1)$$

where $i_{app}(t)$ is the applied current, γ_{Na} is the single-channel sodium conductance, and E_{Na} is the sodium Nernst potential. The number of open sodium channels, $\tilde{n}_{Na}(t)$, is a stochastic process given by

$$\tilde{n}_{Na}(t) = \sum_{j=1}^{N} \tilde{X}_j(t).$$

The $\tilde{X}_j(t)$ are stochastic trajectories defining the open-closed state of channel j at all points in time. If $\tilde{X}_j = 1$, channel j is open; if $\tilde{X}_j = 0$, it is closed.

Each sodium channel consists of a single-channel conductance γ_{Na} in series with the two-state gate $\tilde{X}_j(t)$. Each gate $\tilde{X}_j$ consists of four gating particles, all of which must open for the channel to be open. These four consist of three activation particles $\tilde{m}_{1j}(t)$, $\tilde{m}_{2j}(t)$, $\tilde{m}_{3j}(t)$, and one inactivation particle $\tilde{h}_j(t)$, corresponding to m^3h of the deterministic model. Thus,

$$\tilde{X}_j(t) = \tilde{m}_{1j}(t)\tilde{m}_{2j}(t)\tilde{m}_{3j}(t)\tilde{h}_j(t).$$

Analysis of this model thus requires determination of the trajectories of all four gating particles. This process will be illustrated for a single activation particle.

Assume a "large" population of N two-state particles, $\tilde{m}_j(t)$, alternating randomly between open and closed states.

$$\tilde{m}_j(t) = \begin{cases} 0 & \text{particle } j \text{ closed} \\ 1 & \text{particle } j \text{ open} \end{cases}$$

The mean number of particles in the open state is given by Nm, where m is the probability of any given particle being open. m is determined by the average or expected value of $\tilde{m}_j(t)$, where

$$m(t) = \frac{1}{N}\sum_{j=1}^{N} \tilde{m}_j(t).$$

The behavior of $m(t)$ is determined from the kinetic equation

$$N(1 - m) \underset{\beta_m}{\overset{\alpha_m}{\rightleftharpoons}} Nm,$$

where the rate constants $\alpha_m(V)$ and $\beta_m(V)$ respectively define the mean rates of opening and closing of the particle. This yields

$$\frac{dm}{dt} = \alpha_m(1 - m) - \beta_m m.$$

In the steady-state, $dm/dt = 0$ and the expected value of $\tilde{m}_j$ is given by

$$m_\infty = \frac{\alpha_m}{\alpha_m + \beta_m}.$$

We wish to determine $\tilde{m}_j(t)$, the stochastic open-close trajectory of the specific particle $\tilde{m}_j$ at all points in time. Define the probability distribution function for time of closing, t_c, of an open particle as $P_o(t)$. Then

$$P_o(t) = \Pr(t_c \le t).$$

If we assume that the particles lack memory (open-close transitions are a Markov process), then the open and closed durations have an exponential probability density function (Papoulis, 1984). For a given particle, the kinetics of fluctuation between open and closed are given by

$$\{\tilde{m}_j = 0\} \underset{\beta_m}{\overset{\alpha_m}{\rightleftharpoons}} \{\tilde{m}_j = 1\}.$$

The mean open time of a particle at a given membrane potential V is given by $(\beta_m)^{-1}$ and the mean closed time by $(\alpha_m)^{-1}$. Under voltage-clamp conditions, α_m and β_m are constants. Therefore, the probability distribution functions for particle closing and opening times are given by

$$P_o(t) = 1 - \exp(-\beta_m t), \qquad t \ge 0 \quad (2)$$

$$P_c(t) = 1 - \exp(-\alpha_m t), \qquad t \ge 0 \quad (3)$$

We can determine $P_o(t)$ using the rate constant β_m by noting the probability that the particle closes during interval Δt is given by the conditional probability

$$\Pr\{t_c \le t + \Delta t \mid t_c > t\} = \beta_m(V)\Delta t.$$

Using the formula for conditional probabilities

$$\Pr\{A \mid B\} = \frac{\Pr\{A \cap B\}}{\Pr\{B\}}$$

and allowing $\Delta t \to 0$ gives the differential equation

$$\frac{\dot{P}_o(t)}{1 - P_o(t)} = -\beta_m(V).$$

If we define a specific particle open lifetime $t_o < t < t_c$, where t_o is the time of opening and t_c is the time of closing, this equation is readily solved, giving

$$P_o(t) = 1 - \exp\left\{-\int_{t_o}^{t_c} \beta_m(V(t))\,dt\right\}. \quad (4)$$

The distribution function for particle opening times is determined in the same manner using the opening rate constant α_m:

$$P_c(t) = 1 - \exp\left\{-\int_{t_c}^{t_o} \alpha_m(V(t))\,dt\right\}. \quad (5)$$

Thus, under conditions of time-varying membrane potential, the probability of any given open or closed particle lifetime is drawn from an exponential distribution with a mean value obtained by averaging the rate

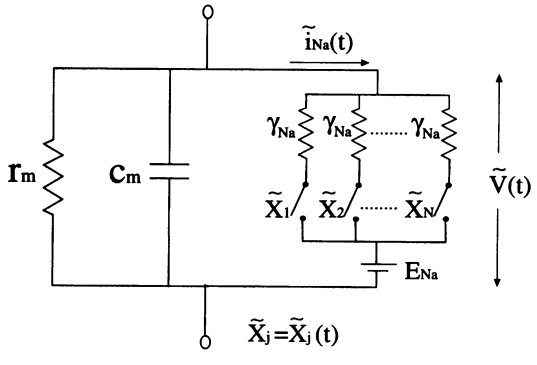

FIGURE 1 Stochastic model for an amphibian node of Ranvier. Each of N voltage-dependent sodium channels has a single-channel conductance γ_{Na}. The instantaneous sodium conductance of the nodal membrane is determined from the product of γ_{Na} and the number of open channels at that time. $\tilde{X}_j(t)$ are the stochastic channel trajectories. If the channel is open $\tilde{X}_j = 1$; if closed $\tilde{X}_j = 0$.

constant over that lifetime. Note that under voltage-clamp, α_m and β_m are constants and Eqs. 4 and 5 reduce to Eqs. 2 and 3. A similar sequence of steps can be performed for an inactivation particle $\bar{h}_j$ using α_h and β_h.

Numerical techniques

Following the methods of Clay and DeFelice (1983), particle lifetime durations are obtained by logarithmic transformation of the output of a uniform random number generator (Press et al., 1992). Initial conditions of each particle are obtained from m_∞ and h_∞ at the resting potential and a sample of $4N$ uniform random deviates. A series of iterations is then begun with 4-μs time steps wherein each particle's state is examined. If a particle is open, the integral Eq. 4 is solved for the closing time, t_c, substituting a uniform random deviate for $\log_e(1 - P_o(t))$. If the particle is closed, integral Eq. 5 is solved for the opening time, t_o, substituting a uniform random deviate for $\log_e(1 - P_c(t))$. The number of open channels $\bar{n}_{Na}(t)$ is determined at that time, and the differential Eq. 1 is iterated one step with an Euler technique. This changes the membrane potential, which alters the rate constants α and β for the subsequent step.

Modeling N sodium channels thus requires following the activity of $4N$ gating particles over 4-μs steps, generating a new uniform deviate every time a particle changes state. Standard model parameters are given in Table 1.

RESULTS

Action potentials

Fig. 2 illustrates the response of a 4000-sodium-channel model to 10 identical near-threshold stimuli. Note that spikes do not always occur and when they do, their timing is random. The standard deviation of spike times is known as jitter. Also note the "noisy" nature of repolarization for both spikes and spike failures. This noise is a manifestation of the random open-close characteristics of a large number of independent activated channels. If the mean of a large number of spikes is obtained, in the limit, the resulting waveform is identical to that produced by the deterministic modified Frankenhauser-Huxley model (SE) illustrated in Fig. 7.

Fig. 3 illustrates the instantaneous number of *open* sodium channels during an action potential for different values of N, the *total* number of sodium channels. With a small number of channels, the stair-step nature of the sodium conductance is apparent and the shape of the conductance curve varies from spike to spike. With larger values of N, the curve becomes smoother, of more consistent shape, and comparable with the variable m^3h in the deterministic model. When N is increased, the passive membrane conductance and capacitance are proportionately increased. N is thus maintained proportionate to the nodal surface area.

TABLE 1 Model fiber parameters at 20°C

Parameter	Symbol	Value	Reference
Axon diameter	d	14.5 μm	Sigworth (1980)
Nodal resistance	R_m	90.9 MΩ	Sigworth (1980)
Nodal capacitance	C_m	1.5 pF	Sigworth (1980)
Number of channels	N	32,000	Sigworth (1980)
Channel conductance	γ_{Na}	10.8 pS	Sigworth (1980)
Resting potential	E_{rest}	−78 mV	Neumcke (1982)
Nernst potential	E_{Na}	74 mV	Schwarz (1987)
Rate constant	α_m	$\frac{0.49(V_m-25.41)}{1-e^{(25.41-V_m)/6.06}}$	Schwarz (1987)
Rate constant	β_m	$\frac{1.04(21-V_m)}{1-e^{(V_m-21)/9.41}}$	Schwarz (1987)
Rate constant	α_h	$\frac{-0.09(27.74+V_m)}{1-e^{(V_m+27.74)/9.06}}$	Schwarz (1987)
Rate constant	β_h	$\frac{3.7}{1+e^{(56-V_m)/12.5}}$	Schwarz (1987)

In the text, when $N < 32{,}000$, membrane properties are scaled assuming a constant channel density per unit nodal area. For the rate constants, membrane potential is offset by the resting potential $V_m = V - E_{rest}$.

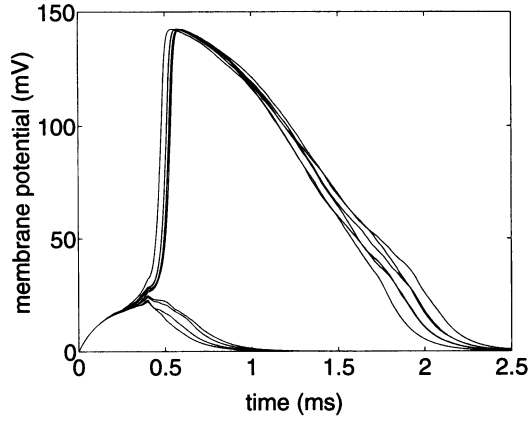

FIGURE 2 Membrane potential response produced by stochastic model to 10 identical near-threshold stimuli. There are 4000 voltage-sensitive sodium channels. Stimuli are 400 μs monophasic rectangular current pulses. Membrane potential is shifted relative to the resting potential.

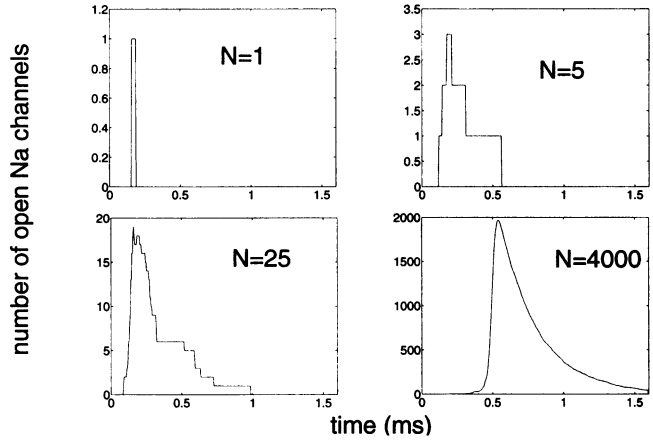

FIGURE 3 Number of open sodium channels during action potential for four different values of N, the total number of voltage-sensitive sodium channels. With increasing N the passive membrane conductance and capacitance are increased proportionately, effectively increasing the nodal surface area. Stimuli are near-threshold, but somewhat greater current densities are required for smaller values of N, resulting in shorter latencies.

Spike timing

Fig. 4 illustrates PST histograms for a 4000-channel model with increasing stimulus intensity. Note that as seen experimentally, latency and jitter both decrease with increasing stimulus intensity. In addition, the histograms are positively

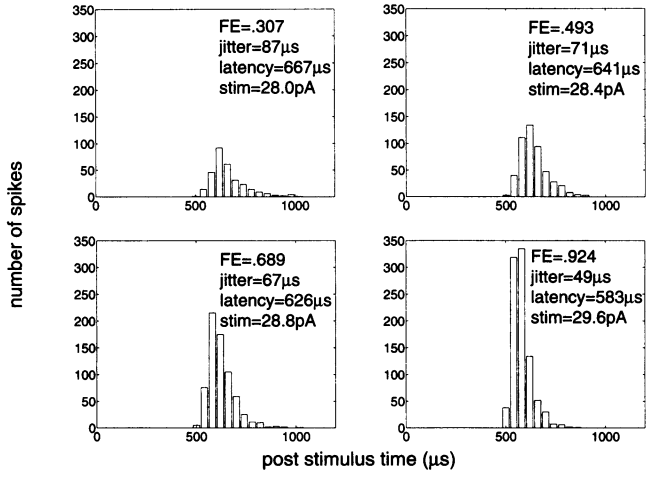

FIGURE 4 PST Histograms at four different stimulus intensities. N = 4000. Firing efficiency (FE) is number of spikes divided by number of stimuli (1000). Latency and jitter are given by the histogram's mean and standard deviation, respectively. Spike time is defined when the membrane potential crosses 75 mV relative to rest, on the upstroke of the action potential.

skewed in the same manner as experimentally obtained histograms, both in frog peripheral nerve (Poussart, 1965; Ten Hoopen and Verveen, 1963; Verveen and Derksen, 1965) and in cat spiral ganglion cells (van den Honert and Stypulkowski, 1984; van den Honert and Stypulkowski, 1987).

Input-output relations

Fig. 5 illustrates input-output functions for three different values of N. As with experimental input-output functions, these are well fit by integrated Gaussians. Note that as N increases, the slope of the function increases. Verveen characterized this slope by the relative spread of threshold (RS), the coefficient of variation of the integrated Gaussian. The RS is obtained by dividing the standard deviation of the Gaussian by its mean. Thus, increasing the number of channels, or presumably the nodal diameter, increases the input-output slope, decreases the RS and results in a less "noisy" node.

Fig. 6 demonstrates the relationship between RS and N. Note that the relationship is approximately linear on a log-log scale. The slope of -0.45 is consistant with a binomial process whose standard deviation is proportional to $N^{-1/2}$. Verveen studied the relationship between fiber diameter and RS in a number of preparations and also found a linear log-log relation.

The relationship between stimulus duration and RS has been studied both experimentally (Poussart, 1965; Verveen and Derksen, 1968) and theoretically (Lecar and Nossal, 1971; Ten Hoopen and Verveen, 1963). For pulse durations between 250 μs and 2.5 ms, there is no change in the RS. Likewise, the stochastic phase-plane calculations of Lecar and Nossal show no dependence of RS on stimulus duration. For the N-channel model, there was no statistically significant change in the RS despite a fourfold change in threshold for rectangular pulses between 100 μs and 3 ms duration. The strength-duration time constant of the model is 320 μs as compared with 309 μs for the underlying deterministic model.

Sensitivity to model parameters

The model parameters have been doubled and halved and the effects on RS and threshold tabulated in Table 2 for N = 4000. For temperature, the numbers reflect the effects of increasing temperature from 20 to 37°C. This reflects only

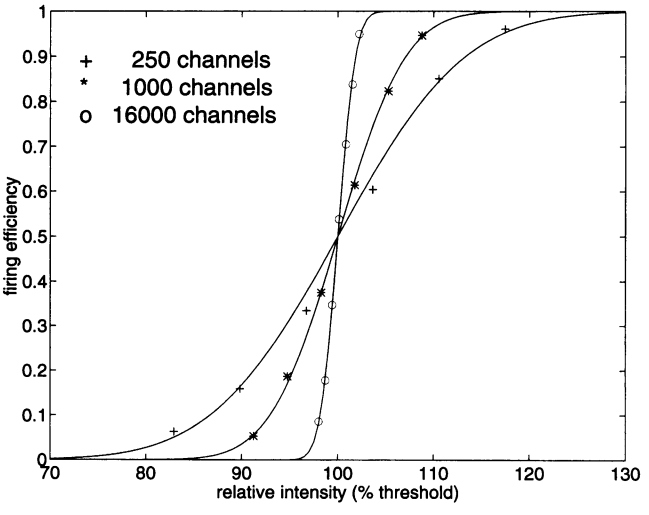

FIGURE 5 Input-Output functions for N = 250, 1,000, and 16,000. With increasing N, there is a steeper slope and a smaller relative spread of threshold (RS).

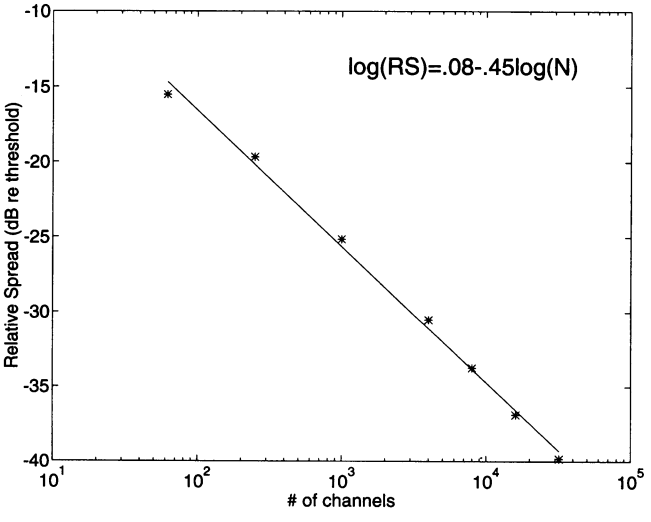

FIGURE 6 Relationship between number of channels, N, and the RS. The equation is a linear fit to the logarithmically transformed data. The slope of -0.45 is consistant with a binomial process whose standard deviation is proportional to $N^{-1/2}$.

TABLE 2 Sensitivity to model parameters for $N = 4000$

Parameter	RS	Threshold
R_m (*2 : *0.5)	+20% : −13%	−39% : +89%
C_m (*2 : *0.5)	−22% : +24%	+35% : −16%
γ_{Na} (*2 : *0.5)	+40% : −30%	−10% : +12%
Temperature (20→37°C)	−24%	−11%

Numbers separated by colons represent the percent change from doubling and halving, respectively, the standard parameter values from Table 1. The results for temperature represent increasing the temperature from 20 to 37°C.

the temperature dependence of the rate constants. The conductances have not been altered so as to illustrate the isolated effects of increasing the rate constants α and β. For activation rate constants, $Q_{10} = 2.2$; for inactivation, $Q_{10} = 2.9$ (Schwarz and Eikhof, 1987). Modeling mammalian nodes will require altering the conductances as well. As noted by Lecar and Nossal, although elevating temperature increases the "noisiness" of individual channels by increasing their open-close rate, the population effect is to decrease RS or the "noisiness" of threshold.

Relation to Frankenhauser-Huxley kinetics

The kinetic equations used to derive the stochastic particle trajectories are obtained from the rat nerve data of Schwarz and Eikhof (1987) at 20°C rather than from the amphibian data of Frankenhauser and Huxley (1964). The original Frankenhauser-Huxley equations include several voltage-dependent conductances, in addition to the sodium conductance, that would significantly increase numerical overhead. To maximize the number of sodium channels that could be represented and the number of stimulus repetitions in the PST histograms, a simplified nodal representation was used. This simplification preserves certain fundamental excitation properties of the original equations as demonstrated in Fig. 7. The similar slope of the spikes' rising edge indicates similar sodium activation rates. The modified model (SE) has a different spike size and duration than the original Frankenhauser-Huxley model (FH), but this would not be expected to cause differences in RS. The membrane capacitance of the SE and FH models are quite similar. The leak conductance of the SE model is approximately twice that of the FH model but from Table 2, this difference would lead to less than a 15% change in the calculated RS. Of greater concern are the sodium channel activation characteristics. Lecar and Nossal have demonstrated that sodium channel activation is a primary determinant of RS. The nearly identical nature of the sodium activation is seen in the similar leading edge of the two action potentials. The validity of this argument could be directly tested by the implementation of an N-channel model of the exact Frankenhauser-Huxley equations. For the modified model, the input-output function for $N = 32{,}000$ required 1 week of computation on a 16-MFlop UNIX workstation. The computational load would be correspondingly increased by the presence of a significant number of voltage-sensitive channels for potassium, and for the nonspecific p current.

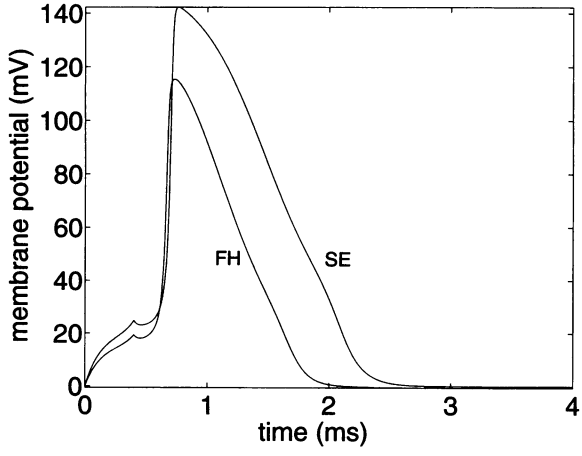

FIGURE 7 Deterministic action potentials produced by the modified (SE) and original (FH) Frankenhauser-Huxley models. Both are with near-threshold stimuli. The similar slope of the spikes' rising edge indicates similar sodium activation rates.

DISCUSSION

A stochastic model of the amphibian node of Ranvier has been presented that is based on the open-close kinetics of single sodium channels. As noted by Clay and DeFelice, the patch-clamp literature provides numerous examples of sodium channels whose microscopic kinetics do not obey Hodgkin-Huxley type equations (Aldrich and Stevens, 1987). The amphibian nodal sodium conductance does appear, however, to have classical microscopic kinetics (Hille, 1992; Wang and Strichartz, 1985). Unitary currents have been recorded from amphibian (Jonas et al., 1989) and human (Scholz et al., 1993) nodal sodium channels, but the exact nature of their microscopic kinetics remains unknown. It is likely, however, that the microscopic kinetics need not be exactly represented to reproduce accurately the macroscopic behavior of the node. It is difficult to distinguish between different kinetic models of a voltage-gated channel with fluctuation analysis, precisely because different kinetic schemes, when averaged over a large number of channels, produce similar macroscopic behavior (Hille, 1992). This argument could be addressed further by incorporating different kinetic analyses into the N-channel model and simulating the macroscopic effect.

This paper demonstrates that a number of experimental observations are reproduced by the N-channel model. In particular, the RS values predicted by the model are consistant with those measured experimentally by Verveen (1962) and by Poussart (1965). Sigworth (1980) has noted that after shrinkage artifact, Verveen's nodal measurement is consistant with fibers 10–12 μm in diameter. Given that Sigworth's representative fiber had a diameter of 14.5 μm and 32,000 sodium channels, and assuming a constant density of channels, Verveen's and Poussart's preparations would have approximately 26,000 sodium channels per node. Using the

relationship in Fig. 6, this corresponds to an RS of 1.2%. Verveen measured a mean RS of 1.1% from 80 fibers, and Poussart reported a mean of 1.6% from 10 fibers. The dependence of RS on the number of channels is similar to the experimentally determined relationship between RS and fiber diameter. The slopes of these functions are different, but the presence of shrinkage artifact makes interpretation of this difference difficult. Note also that Verveen's equation relating RS to fiber diameter was based on three data points each from a different species.

The independence of RS from pulse duration has been noted in several of the aforementioned experimental studies. The *N*-channel model provides a means of testing this independence for very long pulse widths, where stimulus artifact interferes with measurements. Between 100 μs and 3 ms, RS for the model has no statistically significant change.

A relation between temperature and RS was not noted by Verveen or Poussart, but clearly they expected its presence. The analysis of Lecar and Nossal did show a temperature effect on RS of similar magnitude to that reported here. A decrease in RS with increasing temperature has been seen experimentally as well (Erlanger et al., 1941).

It appears that the *N*-channel model adequately predicts certain stochastic properties of spike excitation in the amphibian node. Further comparisons with the experimental literature are in order but await implementation of *N*-channel nodes into a distributed axon model. This will allow prediction of spike jitter, the standard deviation of the PST histogram. Experimental and theoretical work has illustrated a relationship between spike latency, RS and spike jitter (Ten Hoopen and Verveen, 1963; Verveen and Derksen, 1965). Most jitter is thought to arise from the excitation process, but models clearly illustrate that propagation can also affect the magnitude of the jitter (Rubinstein, 1994). Because the latency of a single-node model cannot be compared with experimental data from intact fibers, distributed, multinode models are necessary. Such a model could be of experimental as well as theoretical interest.

Cochlear implants represent an active contemporary application of electrical stimulation. Because the cat auditory nerve has been used extensively in studies of normal hearing, it is a logical choice for single-unit studies of cochlear implants (e.g., Dynes and Delgutte, 1992). With electrical stimulation of the cat spiral ganglion, multiple sites of excitation have been identified (Rubinstein and Dynes, 1993; van den Honert and Stypulkowski, 1984, 1987). These sites demonstrate different strength-duration time constants, thresholds, and jitter. There are possible anatomic correlates for these sites of excitation on the spiral ganglion cell, and extensive morphometric data are available (Liberman and Oliver, 1984). Kinetic data from ionic currents in mammalian spiral ganglion cells are now becoming available (Santos-Sacchi, 1993). By altering the kinetics of the *N*-channel model, it may be possible to study the effects of fiber anatomy on threshold, latency, RS, and jitter.

The primary differences between single-unit responses to acoustic and electric stimuli are related to synchrony. An effort to understand the stochastic mechanisms underlying these differences has potential practical application in developing speech processing strategies for cochlear implants (Finley et al., 1990). Preliminary tests of the model with biphasic and sinusoidal stimuli appear consistent with experimental data regarding the intensity dependence of synchrony.

Sigworth noted the historical relationship between early work with threshold fluctuation and the study of single channels with fluctuation analysis. Clay and DeFelice noted that "the relationship between single channel kinetics and membrane excitability effectively turns the noise problem back to its origins." It may be possible to use macroscopic threshold fluctuation as a tool to study the microscopic nature of the different sites of excitation in intact cells. An obvious example would be to use threshold fluctuation to count sodium channels at the different sites of excitation on the spiral ganglion cell. This would indeed represent a return to the origins of "the noise problem." The success of this approach will depend critically on the absence of significant threshold noise sources other than the microscopic fluctuation of the voltage-sensitive sodium channel.

L. H. Carney, D. K. Eddington, N. Y. S. Kiang, and J. R. Melcher provided much useful criticism of the manuscript. I. F. Garcia-Otero provided expert UNIX system administration. M. W. White introduced me to the work of Verveen. This work was supported by National Institutes of Health program project DC00361.

REFERENCES

Aldrich, R. W., and C. F. Stevens. 1987. Voltage-dependent gating of single sodium channels from mammalian neuroblastoma cells. *J. Neurosci.* 7:418–431.

Blair, E. A., and J. Erlanger. 1933. A comparison of the characteristics of axons through their individual electric responses. *Am. J. Physiol.* 106: 524–564.

Clay, J. R., and L. J. DeFelice. 1983. Relationship between membrane excitability and single channel open-close kinetics. *Biophys. J.* 42:151–157.

DeFelice, L. J. 1981. Introduction to membrane noise. Plenum Press, New York.

Dynes, S. B. C., and B. Delgutte. 1992. Phase-locking of auditory-nerve discharges to sinusoidal electric stimulation of the cochlea. *Hear. Res.* 58:79–90.

Erlanger, J., E. A. Blair, and G. M. Schoepfle. 1941. A study of the spontaneous oscillations in the excitability of nerve fibers, with special reference to the action of strychnine. *Am. J. Physiol.* 134:705–718.

Finley, C., B. S. Wilson, and M. W. White. 1990. Models of neural responsiveness to electrical stimulation. *In* Cochlear Implants: Models of the Electrically Stimulated Ear. J. M. Miller and F. A. Spelman, editors. Springer-Verlag, New York.

Frankenhauser, B., and A. L. Huxley, 1964. The action potential in the myelinated nerve fiber of *Xenopus laevis* as computed on the basis of voltage clamp data. *J. Physiol.* 171:302–315.

Hille, B. 1992. Ionic channels of excitable membranes. Sinauer, Sunderland, MA.

Jonas, P., M. E. Brau, M. Hermsteiner, and W. Vogel. 1989. Single-channel recording in myelinated nerve fibers reveals one type of Na channel but different K channels. *Proc. Natl. Acad. Sci. USA.* 86:7238–7242.

Lecar, H., and R. Nossal, 1971. Theory of threshold fluctuations in nerves. *Biophys. J.* 11:1048–1067.

Liberman, C., and M. E. Oliver. 1984. Morphometry of intracellularly labeled neurons of the auditory nerve: Correlations with functional properties. *J. Comp. Neurol.* 223:163–176.

Neumcke, B., and R. Stampfli. 1982. Sodium currents and sodium-current fluctuations in rat myelinated nerve fibers. *J. Physiol.* 329: 163–184.

Papoulis, A. 1984. Probability, random variables, and stochastic processes, 2nd ed. McGraw-Hill, New York.

Press, W. H., S. A. Teukolsky, W. T. Vetterling, and B. P. Flannery. 1992. Numerical Recipes in Fortran, 2nd ed. Cambridge University Press.

Pecher, C. 1939. La fluctuation d'excitabilité de la fibre nerveuse. *Arch. Int. Physiol. Biochem.* 49:129–152.

Poussart, D. J. M. 1965. Measurement of latency distributions in peripheral nerve fibers. S. M. Thesis. Research laboratory of electronics, Massachusetts Institute of Technology, Cambridge, MA.

Rubinstein, J. T., and S. B. C. Dynes. 1993. Latency, polarity and refractory characteristics of electrical stimulation: Models and single-unit data. *Abstracts of Assoc. Res. Otolaryngol.*

Rubinstein, J. T. 1994. Stochastic properties of electrical stimulation. *Abstracts of Assoc. Res. Otolaryngol.*

Santos-Sacchi, J. 1993. Voltage-dependent ionic conductances of Type I spiral ganglion cells from the guinea pig inner ear. *J. Neurosci.* 13:3599–3611.

Scholz, A., G. Reid, W. Vogel, and H. Bostock. 1993. Ion channels in human axons. *J. Neurophysiol.* 70:1274–1279.

Schwarz, J. R., and G. Eikhof. 1987. Na currents and action potentials in rat myelinated nerve fibers at 20 and 27 degrees. *Pflügers Arch.* 409: 569–577.

Sigworth, F. J. 1980. The variance of sodium current fluctuations at the node of Ranvier. *J. Physiol.* 307:97–129.

Ten Hoopen, M., and A. A. Verveen. 1963. Nerve-model experiments on fluctuation in excitability. *Prog. Brain. Res.* 2:8–21.

van den Honert, C., and P. H. Stypulkowski. 1984. Physiological response properties of the electrically stimulated auditory nerve. II. Single fiber recordings. *Hear. Res.* 14:225–243.

van den Honert, C., and P. H. Stypulkowski. 1987. Temporal response patterns of single auditory nerve fibers elicited by periodic electrical stimuli. *Hear. Res.* 29:207–222.

Verveen, A. A. 1962. Fibre diameter and fluctuation in excitability. *Acta Morphol. Neerland. Scand.* 5:79–85.

Verveen, A. A., and H. E. Derksen. 1965. Fluctuations in membrane potential of axons and the problem of coding. *Kybernetik.* 2:152–160.

Verveen, A. A., and H. E. Derksen. 1968. Fluctuation phenomena in nerve membrane. *Proc. IEEE.* 56:906–916.

Wang, G. K., and G. R. Strichartz. 1985. Kinetic analysis of the action of *Leiurus* scorpion α-toxin on ionic currents in myelinated nerve. *J. Gen. Physiol.* 86:739–762.